Electron scattering by highly polar molecules. I. KI†

M. R. H. Rudge,* S. Trajmar, and W. Williams
California Institute of Technology, Jet Propulsion Laboratory, Pasadena, California 91103
(Received 13 January 1976)

Electron-impact energy-loss spectra of KI were studied experimentally in the 15° to 130° angular range at impact energies of 6.7, 15.7, and 60 eV. The spectra reveal a number of excitation features which have not been detected previously and indicate that KI is a strong photon absorber in the vacuum-uv region. From the spectra, differential and integral electronically elastic and inelastic cross sections have been obtained by normalizing the experimental data to theoretical results at low scattering angles. Rotational excitation cross sections corresponding to $\Delta j = 0, \pm 1$ have been calculated using a dipole-plus-repulsive-core interaction potential and the distorted-wave approximation. For purpose of comparison, the rotational ($\Delta j = \pm 1$) excitation cross sections have also been calculated in the Born point-dipole approximation.

I. INTRODUCTION

The rotational excitation of polar molecules has, since the early work of Massey,[1] received considerable theoretical attention (for reviews see Refs. 2 and 3). Theoretical studies have also been made of the binding properties of dipole systems but conflicting claims have been made concerning the number and nature of the bound states which a polar molecule can support, and what influence the possible bound properties of the system can exert on the scattering process.[4-6] The amount of experimental information is meager. Electron-swarm experiments have been conducted[7-11] but their interpretation is far from clear and has led to conflicting conclusions.[6,12] Negative-ion formation from alkali halides at low-impact energies (resonance capture) has been studied by Ebinghaus.[13] He found that K^-, I^-, KI^-, and K_2I^- were formed with relative probabilties of 1.000, 0.008, 0.035, and 0.038 with appearance potentials of 2.85, 3.20, 3.63, and 3.36 eV, respectively. More recently, single-collision measurements of the scattering of electrons by the strongly polar alkali-halide molecules have been reported.[14-17] The center-of-mass cross sections are not directly obtained from these recoil measurements but a fitting procedure—which need not be unique—has to be applied.[15] Therefore, it is of some interest to conduct direct measurements of the differential cross sections for scattering of electrons by polar molecules in order to eliminate some of the uncertainties in the methods previously used.

The molecule is also of interest from a spectroscopic standpoint. The binding in the ground electronic state is ionic in nature and excitation to a low-lying electronic state corresponds to a transition from an ionic to a covalent bound state. Only a very limited amount of information is available concerning the optical spectrum of KI,[18,19] and to date no electron-impact energy-loss spectrum has been reported. The latter method is especially well suited for detecting optically forbidden excitation and allows the range of optically allowed transitions to be extended into the far uv region.

In this paper we consider the scattering of electrons by the molecule KI, which has a permanent dipole moment of 4.25 a.u. (10.82 D) and should therefore exhibit those characteristics typical of electron scattering by strongly polar species. Electron-impact energy-loss spectra and experimental cross sections for the sum of elastic scattering plus thermal average rotational excitations, and for several electronically inelastic processes are reported. The cross sections have also been calculated in the Born point-dipole approximation ($\Delta j = \pm 1$) and by a distorted wave method ($\Delta j = 0 \pm 1$), which is described in more detail below.

We first review the theoretical background concerning the binding and scattering properties of polar molecules and then describe the experimental technique whereby the energy-loss spectra and cross sections have been obtained. Except where otherwise specified atomic units are used.

II. BOUND-STATE PROBLEM

The dominant interaction between a polar molecule and an electron is that provided by the permanent dipole moment of the molecule. It can be shown[20-22] that a fixed point dipole can support infinitely many bound states if the dipole moment D is greater than 0.639. It can further be shown that the same critical dipole moment holds for a finite dipole or for a dipole plus a spherically symmetric repulsion[23-26] and that a series of critical dipole moments exists for a finite dipole.[27] A polar molecule is not a fixed dipole but has rotational degrees of freedom. Bottcher[28] advanced a proof that the critical moments for a freely rotating di-

pole coincide with those of a fixed dipole. Garrett[29,30,31] however has argued that this proof is invalid since it assumes that the rotational energy levels of the molecule are degenerate. He has calculated the minimum dipole moment necessary to bind an electron to a molecule represented as a rotating finite dipole with nondegenerate energy levels.[31]

Wallis *et al.*[32] have calculated exact energy levels of a fixed dipole but these, partly for the reasons advanced by Garrett,[31] are unlikely to closely approximate the negative-ion affinities of a polar molecule. Crawford[33] has speculated that "any real gas phase molecule or radical with $D \geq 2.0d$ probably can bind an extra electron and almost certainly can if $D \geq 2.5d$." Beyond this there appear to be few theoretical predictions concerning energy levels of the negative ions associated with polar molecules.

There does, however, exist some experimental evidence concerning the affinities of the alkali halides. Ebinghaus[13] has estimated lower bounds to the affinities of a variety of such molecules from measurements of the appearance potential of the molecular negative ion when the neutral dimer is subjected to electron bombardment. His affinity values are typically greater than 1.2 eV. More recently, however, Carlsten *et al.*[34] have conducted photodetachment studies of $LiCl^-$ ($D \approx 3.82$) and find that the affinity is only 0.61 eV, a value somewhat less than half the lower bound of Ebinghaus[13] and about a factor of ten less than the values of Wallis *et al.*[32] On the basis of the more recent measurements we therefore assume that KI^- has an affinity of approximately 0.7 eV.

In considering the scattering problem we adopt a model interaction and choose our model in such a way that it predicts this value for the affinity of KI^-. Constraints imposed by orthogonality requirements are likely to ensure that the radial wave function of the "extra" electron is small within some region typical of the size of the molecule. If r denotes the position vector of the "extra" electron relative to the center of mass of the molecule, it would therefore seem plausible to suppose that the wave function describing this electron is essentially zero for $r < R_0$, where R_0 is some typical molecular dimension. Outside this region the dipole potential is operative and dominates the other multipoles which we neglect. We examine the bound states in this model, described by the Hamiltonian

$$H = -\Lambda^2/2I - \tfrac{1}{2}\nabla_r^2 + V, \tag{1}$$

where I is the moment of inertia of the molecule, Λ^2 is an angular momentum operator, and

$$V = \sum_{\lambda=0}^{1} v_\lambda(r) P_\lambda(\hat{r} \circ \hat{R}), \tag{2}$$

where

$$\begin{aligned} v_0(r) &= \infty, \quad r < R_0 \\ &= 0, \quad r > R_0 \end{aligned} \tag{3}$$

and

$$v_1(r) = -D/r^2. \tag{4}$$

A solution of the Schrödinger equation

$$(H - E)\psi = 0 \tag{5}$$

can be sought in the form

$$\psi = r^{-1} \sum_{jl} y(jlJM \,|\, \hat{R}\hat{r}) F_{jl}^{JM}(r), \tag{6}$$

where y denotes coupled spherical harmonics.

Defining

$$\alpha_j^2 = j(j+1)/I - 2E, \tag{7}$$

it follows that

$$\left(\frac{d^2}{dr^2} - \alpha_j^2 - \frac{l(l+1)}{r^2} \right) F_{jl}^{JM}(r) = \sum_{j'l'} V_{jlj'l'}^{J} F_{j'l'}^{J}(r), \tag{8}$$

where

$$V_{jlj'l'}^{J} = 2 \sum_{\lambda} v_\lambda(r) f_\lambda(jlj'l'J) \tag{9}$$

and the coefficients f_λ are defined by Percival and Seaton.[35] Equation (8) is similar in form to the scattering equations developed by Arthurs and Dalgarno[36] and the bound-state equations of Garrett,[31] the differences lying in the definition of $v_\lambda(r)$.

The infinite set of coupled equation (8) cannot be solved exactly, but in order to obtain an estimate of energy levels we use them as a guide in performing a variational calculation. We consider the case wherein $J = M = 0$ for which triangle conditions demand that $j = l$ and $j' = l'$ and choose a trial function

$$\psi^t = r^{-1} \sum_{i=0}^{N} a_i \, y(l_i l_i 00 \,|\, \hat{R}\hat{r}) \phi_i(r), \tag{10}$$

where

$$l_i = \left[\frac{1+i}{2} \right], \tag{11}$$

and $[x]$ equals the integral part of x. The normalization matrix is

$$N_{ij} = \delta_{l_i l_j} \langle \phi_i, \phi_j \rangle, \tag{12}$$

where angular brackets denote integration. The

Hamiltonian matrix is

$$H_{ij} = -\tfrac{1}{2}\alpha_0^2 N_{ij} - \tfrac{1}{2}\delta_{l_i l_j}\langle\phi_j L_i \phi_i\rangle + \tfrac{1}{2}(\delta_{l_i l_{j+1}} + \delta_{l_i l_{j-1}})\langle\phi_i V_{ij}\phi_j\rangle, \quad (13)$$

where

$$L_i = \frac{d^2}{dr^2} - \alpha_i^2 - \frac{l_i(l_i+1)}{r^2}, \quad (14)$$

and V_{ij} is given by Eq. (9), with $J = l = l_i$, $j' = l' = l_j$, $J = 0$. The eigenvalues E_i are then given by

$$\underline{H} - E_i \underline{N} = 0. \quad (15)$$

The functions $\phi_i(r)$ were chosen by an iterative method which is exemplified for the choice of $N = 1$ by the equations

$$L_0\phi_0^{(n)} = V_{01}\, a_1^{(n-1)}\phi_1^{(n-1)}, \qquad L_1\phi_1^{(n)} = V_{10}\, a_0^{(n-1)}\phi_0^{(n-1)}, \quad (16)$$

the superscripts denoting the order of the iteration. The zeroth-order functions are bounded solutions of the equations

$$L_i\phi_i(r) = 0, \quad (17)$$

and the higher-order iterations were obtained from Eqs. (16) by constructing Green's functions and ensuring that $\phi_i(R_0) = 0$. At each iteration the lowest eigenvalue and the corresponding eigenvector were computed and then inserted on the right-hand side of (16) and the iteration continued until convergence of the eigenvalue was obtained. This was then used to give a new value of α_0 and the process continued. The convergence with respect to N was examined and it was found that $N = 5$ gave results of sufficient accuracy for our purpose. It was found that a value $R_0 = 2.33$ gave rise to an affinity of 0.7 eV.

III. SCATTERING PROBLEM

In treating the scattering of an electron by a polar molecule we make three distinct approximations. The first of these is to neglect the vibrational and electronic channels, the second to model the electron-molecule interaction, and a third approximation is then made in solving the scattering problem within this framework.

Attention has been given to the equation of scattering by a fixed point dipole which can be solved exactly[37] but yields an infinite total cross section.[37,38] Scattering by a fixed finite dipole has also been considered, the equation for which, as in the bound-state problem, separates in prolate spheroidal coordinates.[39,40] This procedure however, when carried through correctly, also yields a divergent total cross section (Garrett[41]).

The earliest treatment employed a rotating point dipole model.[1] This yields finite rotational excitation cross sections but zero elastic scattering cross sections. More complicated potentials have been adopted. For example Crawford and Dalgarno[42] in calculating e^--CO rotational excitation cross sections constructed a model containing six disposable parameters, two for each multipole retained in the potential. A two-parameter model was used by Allison[43] in recent calculations of e^--CsF scattering. While greater flexibility ensues from the use of a multiparameter model it is difficult to establish rigorous criteria whereby all the parameters can be assigned. Therefore we adopt the simple one-parameter model, Eq. (2). This model was used by Rudge[44] who showed that using plane waves gave the model very different results at large scattering angles from those obtained by using plane waves and a point dipole model. The choice of R_0 in those calculations was based on a typical Van der Waals size of a molecule. In the present work we introduce two modifications to this treatment. First we base our choice of R_0 on the predicted value of the KI^- affinity and second we use distorted waves which vanish at R_0 in place of plane waves.

Defining

$$E = k_1^2/2, \quad (18)$$

the scattering by the repulsive core $v_0(r)$ is described by the wave function

$$\psi(\vec{k}_1, \hat{R}, \vec{r}) = (k_1 r)^{-1} Y_{jm_j}(\hat{R}) \times \sum_l i^l (2l+1) l^{i\eta_l} P_l(\hat{k}_1 \cdot \hat{r}) F_l(k_1 r), \quad (19)$$

where

$$F_l(kr) = j_l(kr)\cos\eta_l + n_l(kr)\sin\eta_l \quad (20)$$

and

$$\tan\eta_l = -\, j_l(kR_0)/n_l(kR_0). \quad (21)$$

In these equations, $x^{-1}j_l(x)$ and $x^{-1}n_l(x)$ are regular and irregular spherical Bessel functions, respectively. The elastic scattering is therefore approximately described through the phase shifts η_l.

In order to calculate the inelastic scattering we take a standard variational expression for the scattering amplitude $f_{jj'}(\vec{k}_1, \vec{k}_2)$, where j' is the final rotational quantum number and the energy relation is

$$k_2^2 = k_1^2 + (2I)^{-1}[\, j(j+1) - j'(j'+1)]. \quad (22)$$

The appropriate equation is

$$f_{jj'}(\vec{k}_1,\vec{k}_2) = -(2\pi)^{-1}\int \psi(-\vec{k}_2,\hat{R},\vec{r})(H-E) \times \psi(\vec{k}_1,\hat{R},\vec{r})\,d\vec{r}\,d\hat{R}. \quad (23)$$

After some algebra this reduces to

$$f_{jj'}(\vec{k}_1,\vec{k}_2) = \frac{8\pi D}{9k_1k_2}(-1)^{m_{j'}}[(2j+1)(2j'+1)]^{1/2} \times C^{jj'1}_{000}\sum_{\mu ll'}\exp\{i[\eta_l+\eta'_l+\tfrac{1}{2}\pi(l-l')]\} \times C^{jj'1}_{m_j-m_{j'}\mu}T_{ll'}y(ll'|\mu|\hat{k}_1\hat{k}_2), \quad (24)$$

where

$$T_{ll'} = [(2l+1)(2l'+1)]^{1/2}C^{ll'1}_{000} \times \int_{R_0}^{\infty} r^{-2}F_l(k_1r)F_{l'}(k_2r)\,dr, \quad (25)$$

and C denotes a Clebsch-Gordan coefficient. Series (24) is slowly convergent and it is convenient to define the plane-wave version given by

$$f^P_{jj'}(\vec{k}_1,\vec{k}_2) = 4iD(-1)^{m_{j'}} \times \left(\frac{\pi(2j+1)(2j'+1)}{27}\right)^{1/2}C^{jj'1}_{000}\left(\frac{\sin qR}{q^2R}\right) \times \sum_{\mu} C^{jj'1}_{m_j-m_{j'}\mu}Y_{1\mu}(\hat{q}), \quad (26)$$

where

$$\vec{q} = \vec{k}_1 - \vec{k}_2. \quad (27)$$

The differential cross section is given by

$$\frac{dQ_{jj'}}{d\Omega} = \frac{k_2}{(2j+1)k_1}\sum_{m_jm_{j'}}|f_{jj'}(\vec{k}_1,\vec{k}_2)|^2. \quad (28)$$

The evaluation of (28) proceeds economically by writing

$$f_{jj'}(\vec{k}_1,\vec{k}_2) = f^P_{jj'}(\vec{k}_1,\vec{k}_2) + [f_{jj'}(\vec{k}_1,\vec{k}_2) - f^P_{jj'}(\vec{k}_1,\vec{k}_2)], \quad (29)$$

expression (26) being used for the first term in (29) and partial wave expansions for the second term.

The integral rotational excitation cross section is

$$Q_{jj'} = \int \frac{dQ_{jj'}}{d\Omega}\,d\Omega, \quad (30)$$

and the momentum-transfer cross section is

$$Q^M_{jj'} = \int \frac{dQ_{jj'}}{d\Omega}\left(1-\frac{k_{j'}}{k_j}\cos\theta\right)d\Omega, \quad (31)$$

where θ is the scattering angle.

IV. EXPERIMENTAL MEASUREMENTS

The electron impact spectrometer used to carry out the present measurements has been described elsewhere.[45] An energy selected electron beam of about 50 meV full width at half-maximum was focused onto the KI beam and the scattered-electron intensity was measured as a function of energy loss (ΔE) at fixed impact energies (E_0) of 6.7, 15.7, and 60 eV at fixed scattering angles ranging from 15° to 130°. Energy-loss spectra were obtained by repetitive scanning utilizing pulse counting and multichannel scaling techniques. The KI beam was generated by heating a tantalum crucible, containing KI, by electron bombardment. The impact-energy scale was not calibrated and could be in error by a few tenths of an eV owing to contact potentials. The angular resolution was about ± 2°. Typical spectra are shown in Figs. 1 and 2. From the spectra the relative inelastic scattering intensities with respect to "elastic" scattering were obtained.

In another series of measurements the "elastic" scattering intensity was determined as a function of scattering angle at the three impact energies. During these measurements, the experimental conditions were kept constant and this was confirmed by periodically remeasuring the scattering intensity at 20° and 30° angles. The intensities have been corrected for the variation of "effective path length" with scattering angle by utilizing characteristic correction factors for the geometry of the apparatus. The factors were obtained by measuring the elastic scattering intensities with He and N_2 target beams for which the differential cross sections are known. These correction factors were 0.68, 0.80, and 1.00 at 10°, 20° and 30° (and higher) angles, respectively. The "elastic" scattering intensity includes all elastic, inelastic, and superelastic contributions within the range of instrumental resolution (~ 50 meV). Electronic excitations are well separated but some vibrational excitation (fundamental frequency ≈ 26 meV) may contribute to the thermal average $\Delta j = 0, \pm 1, \pm 2, \ldots$ transitions which we call here (electronically) "elastic" intensity. The procedure for normalization of the differential cross sections and the methods for obtaining integral and momentum transfer cross sections are described in detail below.

Potassium iodide contains about 7% dimers under the conditions of the present experiment[46] and some contribution to the spectra from dimers may be present. Inelastic scattering by atomic potassium is evident in the energy-loss spectra indicating that potassium must also contribute to the observed elastic scattering. The ratio of inelastic to elastic scattering intensities for potassium have been measured[47] and used to give an estimate of the elastic scattering contribution by potassium. At

all energies it was found to be less than 1% of the total signal and has been neglected accordingly.

V. NORMALIZATION PROCEDURE

The theoretical predictions are likely to be at their best at small scattering angles and therefore provide a basis for normalizing the experimental data once the effects arising from a thermal distribution have been corrected.

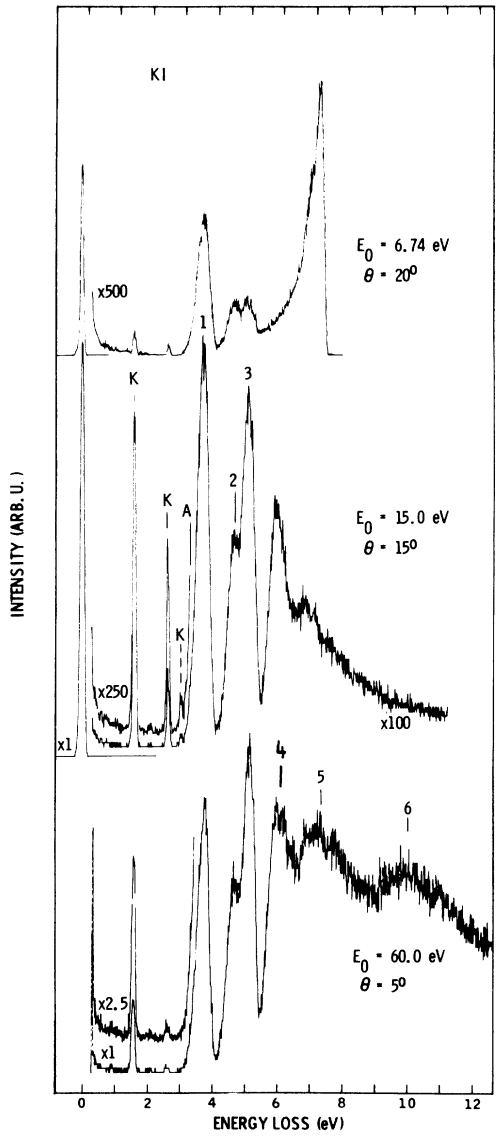

FIG. 1. Electron-impact energy-loss spectra at impact energies E_0 and scattering angles θ as indicated. The features marked by K correspond to excitation of atomic potassium. The symbol A indicates the location of the diffuse optical absorption bands (Ref. 18). The numbers identify prominent peaks (see Table VI).

The dominant contribution to the scattering amplitude at small scattering angles is given by the plane-wave term, Eq. (26). From this it follows that

$$\sum_{j'=j\pm1} \frac{dQ_{jj'}}{d\Omega} \simeq \frac{4D^2k_2}{3q^2k_1}\left(\frac{\sin qR_0}{qR_0}\right)^2. \tag{32}$$

The elastic scattering is small by comparison with the result (32) which therefore represents to a close approximation the small-angle scattering differential cross section for a given initial state j. The quantum number only appears through the momentum transfer $\vec{q}$ which to a close approximation is given by

$$q^2 = 2k_1^2(1-\cos\theta)(1-\delta/k_1)+\delta^2, \tag{33}$$

where

$$\begin{aligned}\delta &= (j+1)/Ik_1, \quad j'=j+1,\\ &= -j/IK_1, \quad j'=j-1.\end{aligned} \tag{34}$$

Since δ is of order 10^{-5} it is apparent that rotational averaging has a negligible effect at angles greater than about 10^{-4} rad.

The zero-angle differential cross section is affected by rotational averaging and we, therefore, examine this assuming a Boltzmann distribution. The thermal average cross section is then very closely given at zero angle by

$$\left\langle\frac{d\sigma}{d\Omega}\right\rangle_{\theta=0} = \frac{\frac{4}{3}(DIk_1)^2\left[1+\sum_{j=1}^{\infty}\frac{(2j+1)}{j(j+1)}\exp\left(-\frac{j(j+1)}{2IkT}\right)\right]}{\sum_{j=0}^{\infty}(2j+1)\exp\left[-\frac{j(j+1)}{2IkT}\right]}, \tag{35}$$

where k is Boltzmann's constant and T is the absolute temperature. If the summations are approximated by integrals this becomes

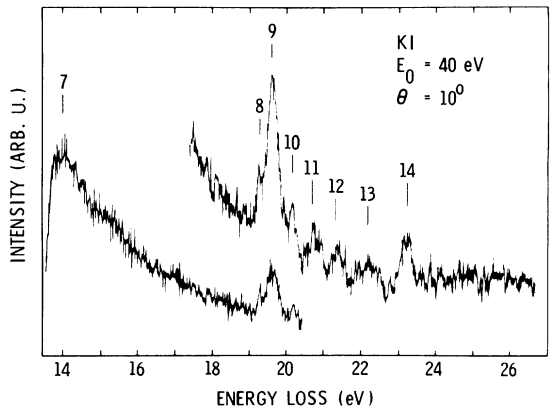

FIG. 2. Energy-loss spectrum at high-energy loss.

$$\left\langle \frac{dQ}{d\Omega} \right\rangle_{\theta=0} = \frac{2(DIk_i)^2}{3IkT}\left[1+E_1\left(\frac{1}{IkT}\right)\right] \quad (36)$$

$$= \left(\frac{dQ}{d\Omega}\right)_{\theta=0} \frac{1}{2}\left[1+E_1\left(\frac{1}{IkT}\right)\right], \quad (37)$$

where $(dQ/d\Omega)_{\theta=0}$ is the zero-angle differential cross section for rotational excitation plus deexcitation from the most probable j state. For $T \approx 1000$ °K we find that

$$\frac{\langle dQ/d\Omega\rangle_{\theta=0}}{(dQ/d\Omega)_{\theta=0}} \approx 4. \quad (38)$$

It follows that the experimental results—if we disregard vibrational excitation—can be normalized to theory at angles of a few degrees without a detailed knowledge of the rotational distribution in the beam. The experimental "elastic"-cross-section curve was normalized to the calculated value of $(dQ/d\Omega)_{\theta=15°}$.

We have also obtained approximate values for the cross sections associated with some of the inelastic features from the intensity ratios and the "elastic" cross sections by multiplying the peak inelastic scattering intensities by a factor of 4.8 to approximately compensate for the width of these features with respect to those of the elastic feature.

TABLE I. Differential cross sections at 6.74 eV (in units of 10^{-16} cm^2/sr). The notation A,n means $A \times 10^n$.

θ (deg)	BPD [a]	Glauber [b]	Experiment [c]	Experiment [d]	Theory [e]
0	1.89, 9	∞	6.33, 9	···	1.89, 9
1	4.49, 4	4.76, 4	3.31, 4	···	4.49, 4
2	1.12, 4	1.21, 4	8.25, 3	···	1.12, 4
3	4.99, 3	5.42, 3	3.65, 3	···	4.97, 3
5	1.80, 3	1.94, 3	1.33, 3	···	1.77, 3
10	4.50, 2	4.24, 2	3.09, 2	···	4.27, 2
15	2.01, 2	···	1.26, 2	1.79, 2	1.79, 2
20	1.13, 2	6.21, 1	6.25, 1	1.06, 2	9.29, 1
25	7.30, 1	2.86, 1	3.36, 1	6.33, 1	5.41, 1
30	5.10, 1	1.44, 1	1.86, 1	4.22, 1	3.39, 1
35	3.78, 1	7.97, 0	1.02, 1	3.07, 1	2.26, 1
40	2.92, 1	5.00, 0	5.25, 0	2.62, 1	1.58, 1
45	2.34, 1	3.52, 0	2.44, 0	2.30, 1	1.18, 1
50	1.91, 1	2.72, 0	8.83, −1	1.99, 1	9.31, 0
55	1.60, 1	2.24, 0	1.71, −1	1.64, 1	7.78, 0
60	1.37, 1	1.89, 0	···	1.25, 1	6.83, 0
65	1.18, 1	1.63, 0	1.77, −1	9.8, 0	6.23, 0
70	1.04, 1	1.40, 0	5.68, −1	9.0, 0	5.83, 0
75	9.23, 0	···	1.08, 0	8.7, 0	5.55, 0
80	8.28, 0	1.03, 0	1.62, 0	8.6, 0	5.33, 0
85	7.49, 0	···	2.17, 0	8.6, 0	5.15, 0
90	6.84, 0	7.61, −1	2.66, 0	8.6, 0	4.98, 0
95	6.29, 0	···	3.06, 0	8.4, 0	4.83, 0
100	5.83, 0	5.68, −1	3.36, 0	8.0, 0	4.69, 0
105	5.43, 0	···	3.57, 0	7.2, 0	4.56, 0
110	5.10, 0	···	3.65, 0	6.3, 0	4.45, 0
115	4.81, 0	···	3.61, 0	5.4, 0	4.35, 0
120	4.56, 0	3.49, −1	3.49, 0	5.1, 0	4.26, 0
125	4.37, 0	···	3.26, 0	5.6, 0	4.19, 0
130	4.16, 0	···	2.96, 0	6.3, 0	4.11, 0
140	3.87, 0	2.55, −1	2.21, 0	···	4.03, 0
160	3.54, 0	2.15, −1	6.7, −1	···	3.93, 0
180	3.42, 0	2.05, −1	···	···	3.90, 0

[a] Born point dipole result, $\Delta j = \pm 1$.

[b] Reference 48 ($D = 4.35$).

[c] Reference 17. Recoil results, include elastic scattering rotational excitation and deexcitation as well as vibrational and electronic excitation.

[d] Present results include elastic scattering, rotational excitation and deexcitation as well as vibrational (but not electronic) excitation.

[e] Present results with $\Delta j = 0, \pm 1$; $j = 75$.

VI. RESULTS

In the calculations we used the values $D = 4.26$, $I = 1.803 \times 10^6$, $R_0 = 2.33$. In Tables I, II, and III we display calculated and measured differential cross sections at impact energies of 6.74 eV, 15.7 eV, and 60 eV. Shown in these tables in the first column are Born point-dipole results (BPD), as presently calculated and in the last column the results obtained by the procedure described previously. The column headed "Glauber" are calculations of Shimamura.[48] The column headed "Experiment[d]" indicates the normalized results of the present measurements and the column headed by "Experiment[c]" represents the recoil data. The differential cross sections are displayed in Figs. 3–5.

In Tables IV and V we show the integral "elastic" and momentum transfer cross sections. The present measurements were extrapolated to 0° (using theoretical values) and to 180° (on the basis of the cross-section curve in the 120°–130° region) to obtain the integral cross sections. These results are displayed in Figs. 6 and 7 where we have assigned error bars of ±25%.

In Table VI we summarize the spectral features which have been observed. It is evident that several strong optical absorption continua exist in the vacuum-uv region for KI and that at high-energy

TABLE II. Differential cross sections at 15.7 eV (in units of 10^{-16} cm^2/sr).

θ (deg)	BPD [a]	Glauber [b]	Experiment [c]	Experiment [d]	Theory [e]
0	4.40, 9	∞	1.77, 10	···	4.40, 9
1	1.93, 4	2.04, 4	1.70, 4	···	1.93, 4
2	4.82, 3	5.17, 3	4.25, 3	···	4.80, 3
3	2.14, 3	2.32, 3	1.88, 3	···	2.12, 3
5	7.72, 2	8.26, 2	6.68, 2	···	7.53, 2
10	1.93, 2	1.81, 2	1.57, 2	···	1.76, 2
15	8.62, 1	···	6.25, 1	7.00, 1	7.00, 1
20	4.87, 1	2.65, 1	2.98, 1	3.57, 1	3.42, 1
25	3.13, 1	1.22, 1	1.52, 1	2.35, 1	1.87, 1
30	2.19, 1	6.13, 0	7.70, 0	2.14, 1	1.12, 1
35	1.62, 1	3.41, 0	3.68, 0	2.10, 1	7.39, 0
40	1.25, 1	2.13, 0	1.51, 0	1.86, 1	5.41, 0
45	1.00, 1	1.50, 0	4.36, −1	1.51, 1	4.38, 0
50	8.22, 0	1.16, 0	3.17, −1	1.12, 1	3.81, 0
55	6.88, 0	9.57, −1	5.39, −2	7.2, 0	3.47, 0
60	5.87, 0	8.10, −1	3.44, −1	5.1, 0	3.23, 0
65	5.09, 0	6.94, −1	7.94, −1	3.5, 0	3.03, 0
70	4.46, 0	5.96, −1	1.32, 0	2.5, 0	2.86, 0
75	3.96, 0	···	1.88, 0	2.0, 0	2.70, 0
80	3.56, 0	4.41, −1	2.42, 0	1.7, 0	2.55, 0
85	3.22, 0	···	2.90, 0	1.7, 0	2.43, 0
90	2.94, 0	3.25, −1	3.31, 0	1.8, 0	2.32, 0
95	2.70, 0	···	3.62, 0	2.0, 0	2.24, 0
100	2.50, 0	2.42, −1	3.82, 0	2.3, 0	2.17, 0
105	2.33, 0	···	3.93, 0	2.5, 0	2.12, 0
110	2.19, 0	···	3.91, 0	2.7, 0	2.08, 0
115	2.06, 0	···	3.82, 0	2.4, 0	2.04, 0
120	1.96, 0	1.50, −1	3.62, 0	2.4, 0	2.01, 0
125	1.87, 0	···	3.34, 0	2.3, 0	1.99, 0
130	1.79, 0	···	3.01, 0	2.0, 0	1.97, 0
140	1.66, 0	1.08, −1	2.20, 0	···	1.94, 0
160	1.51, 0	9.23, −2	6.5, −1	···	1.91, 0
180	1.47, 0	8.75, −2	···	···	1.90, 0

[a] Born point dipole result, $\Delta j = \pm 1$.

[b] Reference 48 ($D = 4.35$).

[c] Reference 17. Recoil results, include elastic scattering rotational excitation and deexcitation as well as vibrational and electronic excitation.

[d] Present results include elastic scattering, rotational excitation and deexcitation as well as vibrational (but not electronic) excitation.

[e] Present results with $\Delta j = 0, \pm 1$; $j = 75$.

losses, well above the ionization limit, several broad features appear. A schematic energy level scheme for KI is shown in Fig. 8. At 6.7-eV impact energy the differential cross sections corresponding to energy losses of 3.7, 4.7, and 5.1 eV are displayed in Fig. 9.

VII. DISCUSSION AND CONCLUSIONS

From Figs. 3–5 and Tables I–III it is evident that there is a considerable disparity both between the theoretical predictions and the experimental results. The most salient feature is that the zero cross section near 60° which is apparent in the recoil measurements is not observed in the present series of measurements. Only at the very high

TABLE III. Differential cross sections at 60 eV (in units of 10^{-16} cm^2/sr).

θ (deg)	BPD [a]	Glauber [b]	Experiment [c]	Theory [d]
0	1.68, 10	∞	···	1.68, 10
1	5.04, 3	5.33, 3	···	5.04, 3
2	1.26, 3	1.35, 3	···	1.26, 3
3	5.61, 2	6.06, 2	···	5.56, 2
5	2.02, 2	2.16, 2	···	1.98, 2
10	5.06, 1	4.74, 1	···	4.61, 1
15	2.25, 1	···	1.82, 1	1.82, 1
20	1.27, 1	6.92, 0	7.55, 0	8.65, 0
25	8.20, 0	3.20, 0	4.60, 0	4.63, 0
30	5.73, 0	1.61, 0	3.16, 0	2.84, 0
35	4.25, 0	8.91, −1	2.11, 0	2.09, 0
40	3.28, 0	5.57, −1	1.46, 0	1.77, 0
45	2.62, 0	3.93, −1	9.8, −1	1.60, 0
50	2.15, 0	3.04, −1	6.1, −1	1.45, 0
55	1.80, 0	2.50, −1	3.6, −1	1.30, 0
60	1.54, 0	2.12, −1	2.1, −1	1.16, 0
65	1.33, 0	1.81, −1	1.2, −1	1.06, 0
70	1.17, 0	1.56, −1	4.3, −2	1.00, 0
75	1.04, 0	···	5.5, −2	9.64, −1
80	9.30, −1	1.15, −1	1.2, −1	9.39, −1
85	8.42, −1	···	1.4, −1	9.15, −1
90	7.68, −1	8.44, −2	2.1, −1	8.90, −1
95	7.07, −1	···	2.9, −1	8.65, −1
100	6.55, −1	6.37, −2	3.6, −1	8.47, −1
105	6.10, −1	···	4.1, −1	8.33, −1
110	5.72, −1	···	4.9, −1	8.24, −1
115	5.40, −1	···	6.4, −1	8.17, −1
120	5.12, −1	3.98, −2	7.7, −1	8.11, −1
125	4.88, −1	···	7.6, −1	8.06, −1
130	4.68, −1	···	7.2, −1	8.00, −1
140	4.35, −1	2.86, −2	···	7.91, −1
160	3.96, −1	2.39, −2	···	7.84, −1
180	3.84, −1	2.23, −2	···	7.82, −1

[a] Born point dipole result $\Delta j = \pm 1$.

[b] Reference ($D = 4.35$).

[c] Present results include elastic scattering, rotational excitation and deexcitation as well as vibrational (but not electronic) excitation.

[d] Present results with $\Delta j = 0, \pm 1$; $j = 75$.

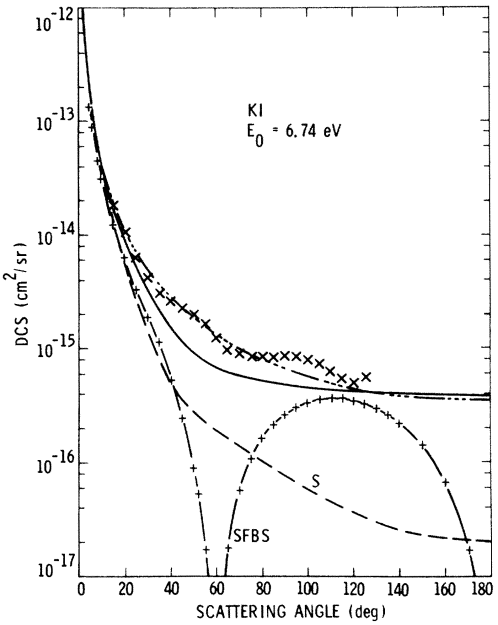

FIG. 3. Differential "elastic" cross sections at 6.7 eV. The symbol × and the curve marked SFBS represent experimental results of the present and the recoil measurements of Ref. 17, respectively. The dot-dash and solid lines are the result of the Born point dipole and the present theory, while the curve marked S is the result of Glauber model (Ref. 48).

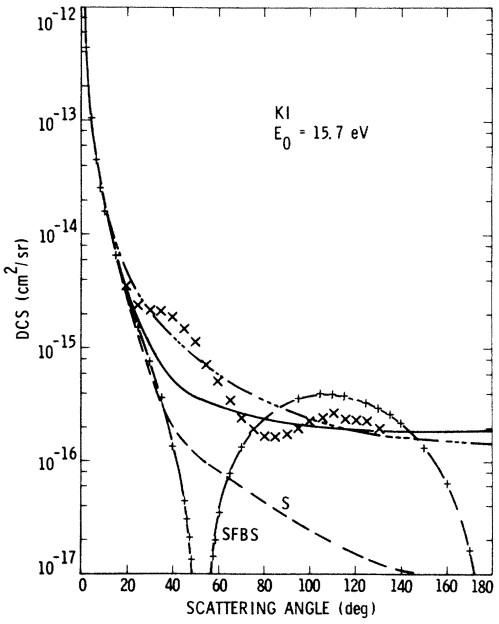

FIG. 4. Same as Fig. 3 except $E_0 = 15.7$ eV.

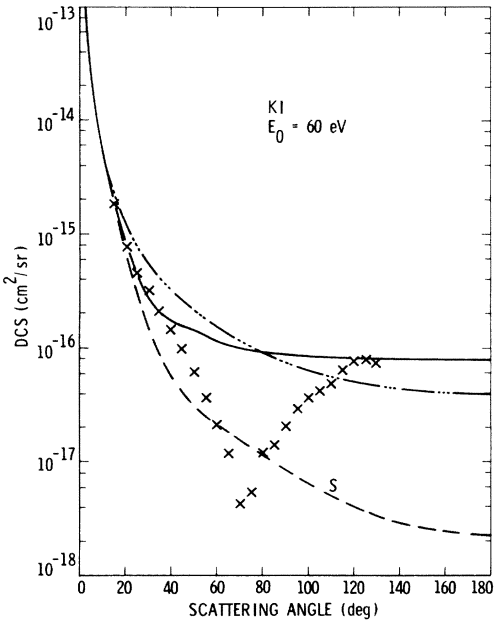

FIG. 5. Same as Fig. 3 except $E_0 = 60$ eV and no recoil data is available for comparison.

energy of 60 eV does any comparable dip appear. This would seem to confirm the idea that this dip is indeed a spurious feature which arises from the numerical techniques used to obtain the differential cross section from the measured molecular recoil. (Note that the units for the differential cross sections given in Fig. 2 of Ref. 17 should be 2π cm^2/sr instead of cm^2.) The zero value at 180° which appears from the recoil measurements is not in agreement with the present theoretical results though the Glauber calculations of Shimamura[48] indicate a small cross section at this angle. It is unlikely, however, that the Glauber approximation has validity in this angular region.

A second, and somewhat surprising, feature which is evident from the figures is that the present measurements show quite close agreement with the Born point dipole results. It is difficult to see that this can be other than fortuitous. If plane waves are used with a model comprising a point dipole plus a repulsive barrier then very different results are obtained.[44] The use of distorted waves and this same model, however, changes the picture to give the present results in which the effect arising from a different scattering approximation partially cancels the effect which arises from a different potential.

A third feature, which is less obvious from the figures, concerns the small-angle behavior of the cross section. In this region we compare the recoil measurements with the present theoretical calculations. In the range 1°–10° and at an impact energy of 6.74 eV the ratio of the present theoretical results to the recoil results is very nearly constant at the value 1.36. At 15.7 eV the same behavior is apparent except that the ratio changes to 1.13. The difference in the 0° results is primarily due to the effect of rotational averaging as discussed in Sec. V. At these angles therefore the shape of the recoil measurements is in harmony with that of the present calculations though they differ by a constant factor. This factor strongly influences the total cross section which is dominated by the small-angle behavior. This accounts for the smaller recoil values displayed in Table IV. We would expect the theoretical results to be most accurate in the small-angle region and the

TABLE IV. Integral "elastic" cross sections (in units of 10^{-16} cm^2).

Energy (eV)	BPD [a]	Experiment [b]	Experiment [c]	Theory [d]
1.0	4.72, 3	···	···	4.57, 3
2.0	2.56, 3	···	···	2.47, 3
4.0	1.38, 3	···	···	1.30, 3
6.7	8.65, 2	5.62, 2	8.43, 2	8.07, 2
8.0	7.41, 2	···	···	6.90, 2
10.0	6.06, 2	···	···	5.63, 2
12.0	5.14, 2	···	···	4.77, 2
14.0	4.47, 2	···	···	4.14, 2
15.7	4.03, 2	3.27, 2	3.92, 2	3.73, 2
60.0	1.18, 2	···	1.08, 2	1.14, 2

[a] Born point dipole result $\Delta j = \pm 1$.

[b] Reference 17. Recoil results, include elastic scattering rotational excitation and deexcitation as well as vibrational and electronic excitation.

[c] Present results include elastic scattering, rotational excitation and deexcitation as well as vibrational (but not electronic) excitation.

[d] Present results with $\Delta j = 0, \pm 1$; $j = 75$.

TABLE V. Momentum transfer cross sections (in units of 10^{-16} cm^2).

Energy (eV)	BPD [a]	Experiment [b]	Experiment [c]	Theory [d]
1.0	5.79, 2	...	...	4.95, 2
2.0	2.90, 2	...	...	2.32, 2
4.0	1.45, 2	...	...	1.12, 2
6.7	8.65, 1	3.27, 1	9.35, 1	6.61, 1
8.0	7.41, 1	...	...	5.60, 1
10.0	5.79, 1	...	...	4.54, 1
12.0	4.83, 1	...	...	3.84, 1
14.0	4.14, 1	...	...	3.34, 1
15.7	3.69, 1	3.31, 1	3.65, 1	3.02, 1
60.0	9.65, 0	...	7.90, 0	1.15, 1

[a] Born point dipole result $\Delta j = \pm 1$.

[b] Reference 17. Recoil results, include elastic scattering rotational excitation and deexcitation as well as vibrational and electronic excitation.

[c] Present results include elastic scattering, rotational excitation and deexcitation as well as vibrational (but not electronic) excitation.

[d] Present results with $\Delta j = 0, \pm 1$; $j = 75$.

apparent difference between theory and recoil experiment here is difficult to reconcile. The Glauber calculations give rise to the surprising conclusion that the elastic scattering cross section is infinite at zero angle,[49] though the singularity is integrable. Between about 5° and 35° the Glauber results are close to the recoil values but otherwise there is little agreement with either set of experimental results. The present experimental and calculated "elastic" differential cross-section curves have a similar angular behavior. This fact and the normalization of the experimental data to theory at 15° results in the good agreement in the integral cross sections. The disagreement among the various data at high angles reflects in the momentum transfer cross sections.

A few general remarks can be made concerning the energy-loss spectra, the electronic energy level scheme, and the inelastic cross sections.

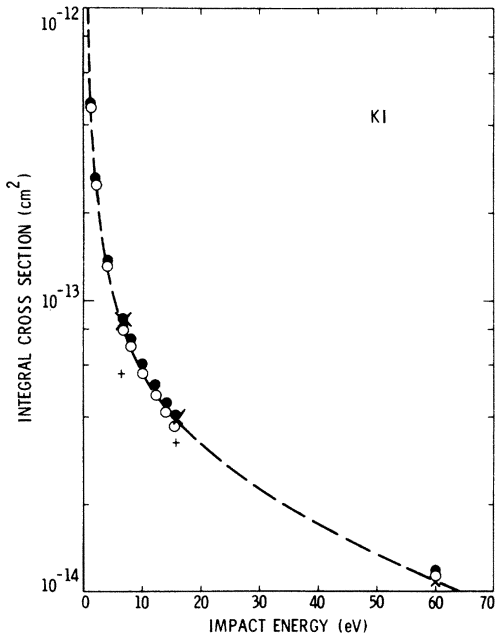

FIG. 6. Integral "elastic" cross sections as function of impact energy. The symbols ● and ○ refer to the results obtained from the BPD and from the present theory, respectively. The symbols × and + represent experimental data from the present and from the recoil measurements respectively. A line which represents the cross sections in this energy range was drawn through these points.

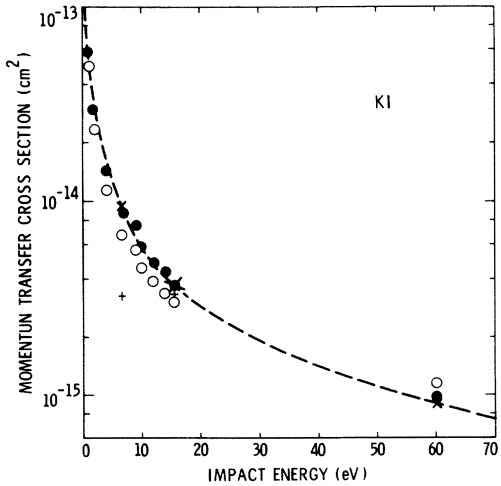

FIG. 7. Momentum-transfer cross sections as a function of impact energy. The symbols have the same meaning as in Fig. 6.

TABLE VI. Summary of spectral features.

Feature [a]	Excitation energy (eV) [b] Optical [c]	Electron impact [d] $E_0 = 60$ eV	$E_0 = 6.7$ eV
A	3.32	...	...
1	3.81	3.80	3.72
2	4.75	4.72	4.64
3	5.29	5.15	5.04
4		6.15	
5		7.3	
6		9.9	
7		14.0	
8		19.2	
9		19.6	
10		20.1	
11		20.7	
12		21.3	
13		22.2	
14		23.3	

[a] Designation used in Figs. 1 and 2.
[b] Corresponds to optical absorption peak or electron scattering peak.
[c] Reference 18.
[d] Present results.

It is known that the optical spectrum of KI consists of a number of diffuse bands at about 3.3 eV which blend into a continuum at around 3.5 eV and that two additional continua have been observed at 4.75 and 5.29 eV.[18,19] No assignments have been made for any of these transitions. In the electron impact energy-loss spectra of Fig. 1 the diffuse bands are not apparent. It would require higher resolution and longer scanning time to reveal them. The three optical absorption continua appear strongly. Going from 60 to 6.7 eV impact energy, the position of these peaks shift about 0.1 eV toward lower energy losses (see Table VI) indicating the presence of optically forbidden, possibly spin exchange transitions. It is tempting to associate the 3.32, 3.72, and 3.80 eV features with the $^1\Sigma^+$, $^3\Pi$, and $^1\Pi$ excited states and in a similar manner the 4.64, 4.72, 5.04, and 5.15 eV features with the next group of $^3\Sigma^+$, $^1\Sigma^+$, $^3\Pi$, and $^1\Pi$ states, respectively. Strong broad excitation features appear at 6.2, 7.3, 7.9, and 14 eV energy losses (Fig. 1, 60-eV spectrum) revealing that KI is a strong absorber in the vacuum-uv region. At energy losses over 19 eV several additional features are present (Fig. 2). None of these transitions can be assigned at the present. A schematic representation of what is known about the energy levels of KI and KI^- is shown in Fig. 8. The dissociation limits are based on the dissociation energy of ground state KI, [18] and on the energy levels, [50] ionization potentials, and electron affinities of K and I. [51] The molecular states obtained from the separated atoms, assuming Hund's coupling case a, [18] are indicated on the tentative potential energy curves. The energy levels corresponding to the observed features A–4 (Table VI) are indicated in the Franck-Condon region. The KI^- curves in the same region are located at – 0.7, 2.85, and 3.20 eV on the basis of the estimated electron affinity of KI ground state and the appear-

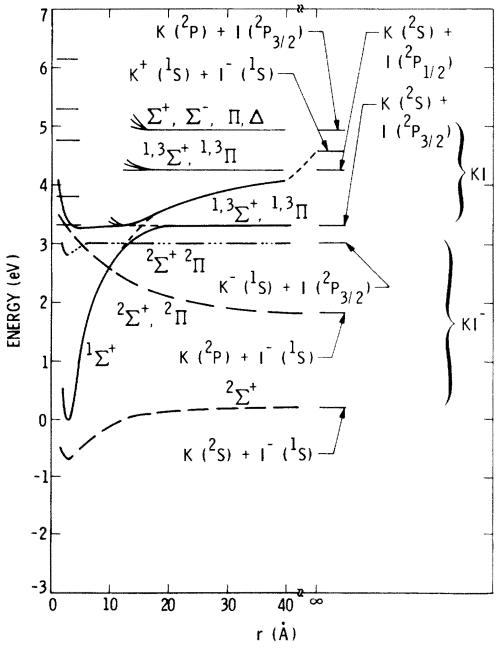

FIG. 8. Schematic energy-level diagram and potential-energy curves for KI and KI^-.

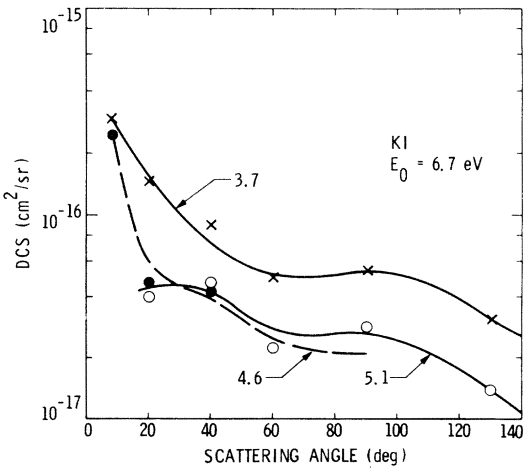

FIG. 9. Differential cross sections for the broad inelastic features located at 3.7, 4.7, and 5.1 eV energy losses.

ance potentials for I^- and K^-, respectively.[13] The crossing between the ionic ground and covalent excited $^1\Sigma^+$ states for alkali halides has been discussed previously.[52-54] The inelastic differential cross sections are large compared to other diatomic molecules (N_2, O_2, CO, NO) which have much smaller or no permanent dipole moments.

We conclude that further experimental and theoretical effort is needed before electron–polar-molecule scattering is well understood. The model potential that we have used can be improved upon though it has the virtue that it contains no free parameters once the affinity has been determined. The scattering approximation is probably fairly good so far as the integral cross sections are concerned, though it may be insufficiently accurate to reveal details of the differential cross section. The effects arising from other processes, such as vibrational excitation or dissociative attachment, have been completely ignored. Associated with these latter processes there is the possibility of resonance and threshold effects which demand further experimental and theoretical study.

ACKNOWLEDGMENTS

We would like to thank Dr. R. Stern for sending us the tabulated results of the recoil work and Dr. Shimamura and Professor Takayanagi for giving us the results of their calculations prior to publication. One of the authors (S.T.) is grateful for valuable discussions with Professor R. S. Berry and Professor O. Crawford.

---

*Permanent address: Dept. of Applied Mathematics and Theoretical Physics, The Queen's University of Belfast, Northern Ireland.

†Supported in part by the National Aeronautics and Space Administration under Contract No. NAS7-100 to the Jet Propulsion Laboratory and in part by the U. S. Office of Naval Research under Contract No. N00014-69-C-0035 to the Queen's University of Belfast.

[1]H. S. W. Massey, Proc. Camb. Philos. Soc. 28, 99 (1931).
[2]K. Takayanagi and Y. Itikawa, Adv. At. Mod. Phys. 6, 105 (1970).
[3]K. Takayanagi, Comments At. Mol. Phys. 3, 95 (1972).
[4]J. M. Lévy-Leblond and J. P. Provost, Phys. Lett. 26b, 104 (1967).
[5]O. H. Crawford, A. Dalgarno, and P. B. Hays, Mol. Phys. 13, 181 (1967).
[6]A. Dalgarno, O. H. Crawford, and A. C. Allison, Chem. Phys. Lett. 2, 381 (1968).
[7]N. Hamilton and J. A. D. Stockdale, Aust. J. Phys. 19, 813 (1966).
[8]L. G. Christophorou, G. S. Hurst, and W. G. Hendrick, J. Chem. Phys. 45, 1081 (1966).
[9]L. G. Christophorou, G. S. Hurst, and A. Hadjiantoniou, J. Chem. Phys. 44, 3506 (1966).
[10]L. G. Christophorou and A. A. Christoulides, J. Phys. B 2, 71 (1969).
[11]L. G. Christophorou and G. Pittman, J. Phys. B 3, 1252 (1970).
[12]J. A. D. Stockdale, L. G. Christophorou, J. E. Turner, and V. E. Anderson, Phys. Lett. 25A, 510 (1967).
[13]H. Ebinghaus, Z. Naturforsch. 19A, 727 (1964); English translation available as Air Force Cambridge Research Laboratories Report AFCRL-68-0482 (Translation No. 2).
[14]R. C. Slater, M. G. Fickes, W. G. Becker, and R. C. Stern, J. Chem. Phys. 60, 4697 (1974).
[15]M. G. Fickes and R. C. Stern, J. Chem. Phys. 60, 4710 (1974).
[16]W. G. Becker, M. G. Fickes, R. C. Slater, and R. C. Stern, J. Chem. Phys. 61, 2283 (1974).
[17]W. G. Becker, M. G. Fickes, R. C. Slater, and R. C. Stern, J. Chem. Phys. 61, 2290 (1974).
[18]G. Herzberg, *Molecular Spectra and Molecular Structure I. Spectrum of Diatomic Molecules* (Van Nostrand, Princeton, N.J., 1950).
[19]H. Levi, dissertation (Berlin, 1934) (unpublished).
[20]A. S. Wightman, Phys. Rev. 77, 521 (1950).
[21]J. E. Turner and K. Fox, Phys. Lett. 23, 547 (1966).
[22]M. H. Mittleman and V. P. Myerscough, Phys. Lett. 23, 545 (1966).
[23]J. M. Lévy-Leblond, Phys. Rev. 153, 1 (1967).
[24]W. B. Brown and R. E. Roberts, J. Chem. Phys. 46, 2006 (1967).
[25]O. H. Crawford and A. Dalgarno, Chem. Phys. Lett. 1, 23 (1967).
[26]O. H. Crawford, Proc. Phys. Soc. Lond. 91, 279 (1967).
[27]C. A. Coulson and M. Walmesley, Proc. Phys. Soc. Lond. 91, 31 (1967).
[28]C. Bottcher, Mol. Phys. 19, 193 (1970).
[29]W. R. Garrett, Chem. Phys. Lett. 5, 393 (1970).
[30]W. R. Garrett, Mol. Phys. 20, 751 (1971).
[31]W. R. Garrett, Phys. Rev. A 3, 961 (1971).
[32]R. F. Wallis, R. Herman, and H. W. Milnes, J. Mol. Spectros. 4, 51 (1960).
[33]O. H. Crawford, Mol. Phys. 20, 585 (1971).
[34]J. L. Carlsten, J. R. Peterson, and W. C. Lineberger, *Abstracts on the Papers on the Ninth International Conference on the Physics of Electronic and Atomic Collisions*, edited by J. S. Risley and R. Geballe (University of Washington Press, Seattle, 1975), p. 379.
[35]I. C. Percival and M. J. Seaton, Proc. Camb. Philos. Soc. 53, 654 (1957).
[36]A. M. Arthurs and A. Dalgarno, Proc. R. Soc. A 256, 540 (1960).
[37]M. H. Mittleman and R. E. Von Holdt, Phys. Rev. 140, A726 (1965).
[38]N. F. Mott and H. S. W. Massey, *The Theory of Atomic Collisions*, 3rd ed. (Oxford U. P., London, 1965).
[39]M. Shimizu, J. Phys. Soc. Jpn. 18, 811 (1963).
[40]K. Takayanagi and Y. Itikawa, J. Phys. Soc. Jpn. 24,

160 (1968).
[41]W. R. Garrett, Phys. Rev. A 4, 2229 (1971).
[42]O. H. Crawford and A. Dalgarno, J. Phys. B 4, 494 (1971).
[43]A. C. Allison, J. Phys. B 8, (1975).
[44]M. R. H. Rudge, J. Phys. B 7, 1323 (1974).
[45]W. Williams and S. Trajmar, Phys. Rev. Lett. 33, 187 (1974).
[46]R. C. Miller and P. Kusch, J. Chem. Phys. 25, 860 (1965).
[47]W. Williams and S. Trajmar (unpublished).
[48]I. Shimamura (private communication).
[49]O. Asihara, I. Shimamura, and K. Takayanagi, J. Phys. Soc. Jpn. 38, 1732 (1975).
[50]C. E. Moore, *Atomic Energy Levels*, NBS Circ. No. 467 (U.S. GPO, Washington, D.C., 1958).
[51]C. E. Melton, *Principles of Mass Spectrometry and Negative Ions* (Marcel Dekker, New York, 1970).
[52]E. J. W. Verwey and J. H. DeBoer, Recl. Trav. Chim. Pays-Bas 55, 431 (1956).
[53]R. S. Berry, J. Chem. Phys. 27, 1288 (1957); 54, 1752 (1971).
[54]L. R. Kahn, P. J. Hay, and I. Shavitt, J. Chem. Phys. 61, 3530 (1974).